X-693-75-256
PREPRINT

NASA TM X- 70990

NEW SOURCE LOCATION MEASUREMENTS OF TERRESTRIAL KILOMETRIC RADIATION

(NASA-TM-X-70990) NEW SOURCE LOCATION MEASUREMENTS OF TERRESTRIAL KILOMETRIC RADIATION (NASA) 18 p HC $3.25 CSCL 08N

N75-33556

Unclas
G3/46 39006

M. L. KAISER
J. K. ALEXANDER

OCTOBER 1975

GSFC

GODDARD SPACE FLIGHT CENTER
GREENBELT, MARYLAND

NEW SOURCE LOCATION MEASUREMENTS OF TERRESTRIAL KILOMETRIC RADIATION

M.L. Kaiser and J.K. Alexander
Radio Astronomy Branch
Laboratory for Extraterrestrial Physics
Goddard Space Flight Center
Greenbelt, Maryland 20771

Abstract

Two dimensional source locations of individual terrestrial kilometric radiation (TKR) events have been measured by the Radio Astronomy Explorer-2 (RAE-2) spacecraft in lunar orbit. Although the average source location is above the polar regions near the Earth (r ~2-3 R_E), there are a significant number of events which occur at > 7 R_E from the Earth. Furthermore, there is considerable evidence for multiple sources and source motion over the time scale of tens of minutes. Recent TKR mechanism theories which assume that the emission occurs at or near the local electron gyrofrequency would predict generation much closer to the Earth's surface. We therefore suggest that alternative emission mechanisms (other than gyroemission) are required to explain all TKR events.

INTRODUCTION

During the past few years, several investigators have obtained measurements of intense kilometer wavelength radio emissions (TKR for terrestrial kilometric radiation) emanating from the Earth's auroral magnetosphere (Dunckel et al., 1970; Gurnett, 1974; Kaiser and Stone, 1975; Kurth et al., 1975). A number of theoretical models for these emissions have also been developed (Gurnett, 1974; Benson, 1975; Melrose 1975). Although each theory cited differs in detail from the others, a' e similar in that they predict emission at or near the local electron gyrofrequency or its low-order harmonics. Hence, these models imply generation of the radiation relatively near the Earth's surface. For example, at 250 kHz where TKR events most often have a spectral peak, these theories would have the source of emission located at altitudes less than 2.0 R_E.

We have determined source locations using lunar occultations of the Earth as viewed by the Radio-Astronomy-Explorer-2 (RAE-2) spacecraft. This technique yields a two-dimensional map of the source location rather than the one-dimensional ecliptic plane projections reported by previous investigators. The inherently high accuracy of this occultation method also enables the source location of individual events to be studied on a time scale of tens of minutes. We find that the long term average source location close to the Earth

reported in the previous papers may be misleading. We observe a large number of events that are situated much further from the Earth than "gyroemission" theories would predict. In addition we find evidence for source motion, and we have observed several TKR events that can be explained only in terms of multiple sources emitting simultaneously. In view of the dynamical complexity of the TKR phenomenon, emission mechanisms other than, or in addition to, gyroemission may be necessary to understand TKR.

METHOD AND OBSERVATIONS

The RAE-2 spacecraft was placed in lunar orbit in June, 1973. It carries radio receivers capable of monitoring emission at intensity levels as low as cosmic background over a 32-channel band from 25 kHz to 13 MHz. The technical details of the spacecraft have been published by Alexander et al. (1975) and will not be further described here. Approximately every two weeks, a seven-day series of lunar occultations of the Earth begins. The occultations occur on each 222-minute orbit, and individual occultations can last up to 48 minutes.

Figure 1 illustrates the technique of deriving two-dimensional source position measurements from a lunar occultation event. The signal intensity at 250 kHz is plotted against time in the lower panel, and the period of occultation of the visible Earth is indicated by the

horizontal bar. We measure the time at which the signal first begins to disappear, t_1, and the time at which the signal has completely reappeared, t_4. Times t_2 and t_3 are the points at which the signal is reduced to 10% of its full value. These four times are then used to define the source position as shown in the upper panel. The Earth is drawn as it would be seen from the Moon at the time of the occultation showing the position of the geomagnetic pole visible from the Moon and the terminator separating the day and night hemispheres. The series of long arcs are projections of the position of the Moon's limb at the indicated times onto the plane perpendicular to the line of sight. The area bounded by the four measured times contains the source as projected onto this plane. Since this is a projection, it will give a minimum separation of the actual source from the Earth. The errors in this method due to uncertainties in defining the four limb encounter times and uncertainies in the ephemeris data are estimated to be less than $\pm 1/2\ R_E$ for most events. A consistency check of the method can often be made by noting the measured position of groundbased transmissions, primarily man-made or thunderstorm noise, at frequencies $\gtrsim$ 4 MHz. In the case of these events $t_1 \cong t_2$ and $t_3 \cong t_4$, so the method yields a single point on the Earth's disk. For the event shown in Figure 1, the high-frequency noise disappeared

at 1851.5 and reappeared at 1927 which would place the source on the dark hemisphere. Significant timing errors would place the measured high-frequency position off the disk.

We have now examined nearly six months of Earth occultation data covering the period July - December, 1973. Figures 2a,b and c are examples of some of the source position results that have led us to question the current theoretical interpretations of TKR. The format for each figure is similar. Gurnett (1974) showed that the TKR is correlated with particle precipitation events in the auroral zones which are in turn correlated with the auroral electrojet (AE) index. Thus, the bottom panel in each figure shows the hourly average value of AE in units of gammas for the indicated dates and times. Superimposed on each AE plot are bars indicating the times at which Earth occultations took place. For each figure the resulting RAE-2 source occultation positions deduced for 250 kHz are shown in the upper panels. In all three figures, the observations were taken when the Moon was near first quarter so that RAE-2 was situated over the dusk meridian of the Earth. Consequently, the measured positions are projected onto the noon-midnight meridian plane.

Figure 2a shows three occultation events on Aug 3-4, 1973. All three occultations happen to occur near the maximum phase of geomagnetic

substorms as inferred from AE. Only event number 2 at 10 hours UT is completely consistent with an electron gyrofrequency explanation. Even 3 occurs at a geocentric distance of $>3\ R_E$ while event number 1 is a double source (two distinct steps during the occultation) with one component projected onto the disk of the Earth and another at $>15\ R_E$.

Figure 2b shows five source locations measured on October 6, 1973. The events at about 1,5,9 and 16 hours UT all occur during some phase of a substorm and the resulting source locations are all beyond 3 R_E geocentric distance. The event at 12 hours occurs during a magnetically quiet period with $AE \cong 40\gamma$. The source for this event occupies a small region just above the North magnetic pole, well within the bounds of the gyrofrequency theories. The source observed at 16 hours at a time corresponding to the expansion phase of a substorm has apparently moved away from the polar region to a position near the nighttime equator.

Figure 2c shows observations from November 2, 1973, when AE was seldom less than 200γ indicating considerable auroral activity. With the exception of the event near 15 hours UT, all source locations are at large geocentric distances ($>4R_E$) above the Northern (nighttime) auroral zone. The occultation event at 15 hours was very complex and

gave an apparent source position projected above the southern hemisphere. None of the events on this day fall within the bounds of the gyroemission theories.

The examples shown in figure 2 were chosen obviously to emphasize our point concerning the altitude of the emission regions. Source positions like the one at 12 hours on October 6, 1973 (figure 2a) are, to be sure, common. These events occur during quiet periods, and since AE was below 100 γ about 37% of the time during our observing interval, (July-December, 1973) is it not surprising that we also recorded many " well behaved" events. However, events beyond the relevant gyrofrequency altitude are not rare. Figure 3 shows the distribution of projected geocentric distances for all 112 events measured at 250 kHz during the observing interval. The average distance is 3.4 R_E, which is beyond the largest distance any of the current theories would predict. Moreover, fully 1/3 of our events are beyond 3.5 R_E and 10% are beyond 7.0 R_E, well above the 250 kHz gyrofrequency level or its low-order harmonics. Clearly some emission mechanism other than those currently proposed must be invoked to explain a substantial fraction of the TKR source locations.

We would like to emphasize that the one-dimensional source maps done by Gurnett (1974), Kaiser and Stone (1975) and Kurth et al. (1975) are not incorrect but, rather, incomplete. We can simulate

such a one-dimensional map with our measured two-dimensional source locations. We have projected the source direction for each event onto the ecliptic plane and then proceeded to intersect these source direction lines in the same manner as Kaiser and Stone (1975). Figure 4 is the ecliptic plane projection of the distribution of intersections displayed on a local time versus radial distance grid. This plot compares remarkably well with figure 1b of Kaiser and Stone (1975) and figures 5 and 9 of Kurth et al. (1975). All of these one-dimensional plots show a major source region in the pre-midnight sector at about 1.0 - 1.5 R_E geocentric distance. This near-Earth source location results in part from lack of two-dimensional information. As can be seen from figures 2a,b and c, many events occur at large distances above the magnetic poles, but the direction determination methods used in the earlier studies were sensitive only to angular separations in the ecliptic plane. Furthermore, the earlier studies depended on measurements of the mean position over rather long periods of time (≥ 10 hours). However the occultation data show that there can be considerable motion over the time interval of tens of minutes. It is easy to see how theorists using the time-averaged source location maps might postulate a gyrofrequency mechanism.

The implications of these large source location distances may go beyond just the few theories concerned with TKR. Kaiser and Stone (1975) mentioned several similarities between the radio emissions of Earth and Jupiter. If these similarities extend to the physical mechanisms involved in the emission, then Jovian decametric radiation theories may need to be revised because most of these theories (see Smith, 1976) also invoke some form gyroemission.

ACKNOWLEDGEMENT

The authors express thanks to Dr. J. Fainberg for providing the coordinate transformations necessary to produce figures 1 and 2, and to Mrs. P. Harper and S. Vaughan for their assistance in the data processing.

References

Benson, R.F., Source Mechanism for Terrestrial Kilometric Radiation, Geophys. Res. Lett., 2, 52-55, 1975.

Dunckel, N., B. Ficklin, L. Rorden, and R.A. Helliwell, Low-Frequency Noise Observed in the Distant Magnetosphere with OGO 1, J. Geophys. Res., 75, 1854-1862, 1970.

Gurnett, D.A., The Earth as a Radio Source: Terrestrial Kilometric Radiation, J. Geophys. Res., 79, 4227-4238, 1974.

Kaiser, M.L., and R.G. Stone, Earth as an Intense Planetary Radio Source: Similarities to Jupiter and Saturn, Science, 189, 285-287, 1975.

Kurth, W.S., M.M. Baumback, and D.A. Gurnett, Direction-Finding Measurements of Auroral Kilometric Radiation, J. Geophys. Res., 80, 2764-2770, 1975.

Melrose, D.B., An Interpretation of Jupiter's Decametric Radiation and the Terrestrial Kilometric Radiation as Direct Amplified Gyro-Emission, preprint, 1975.

Smith, R.A., Models of Jovian Decametric Radiation, to appear in Jupiter, The Giant Planet, T. Gehrels ed., Univ. of Arizona Press, Tucson, Arizona, 1976.

FIGURE CAPTIONS

Figure 1. An example of an occultation of TKR observed by the RAE-2 spacecraft at 250 kHz. The four "contact" times of the occultation (lower panel) define the source region as shown in the upper panel. The bar in the lower panel indicates the duration of the occultation of the visible Earth.

Figure 2. (Upper panel) Examples of RAE-2 lunar occultation positions of TKR sources projected onto the plane perpendicular to the Earth-Moon line. The vertical axis is aligned along the projection of the Earth's magnetic axis. The locations derived for the source of high frequency emissions from near the Earth's surface on Nov. 2, 1973 are indicated by an *. (Lower panel) Plots of the hourly average of the AE index for the period of the occultation measurements. The times of each occultation event are indicated by the vertical bars.

Figure 3. The distribution of projected radial positions (minimum distance) of TKR emission at 250 kHz during the period July-December, 1973 as measured by RAE-2.

Figure 4. Contours of the relative occurrence of 250 kHz TKR source positions projected onto the ecliptic plane in a local time versus radial distance grid.

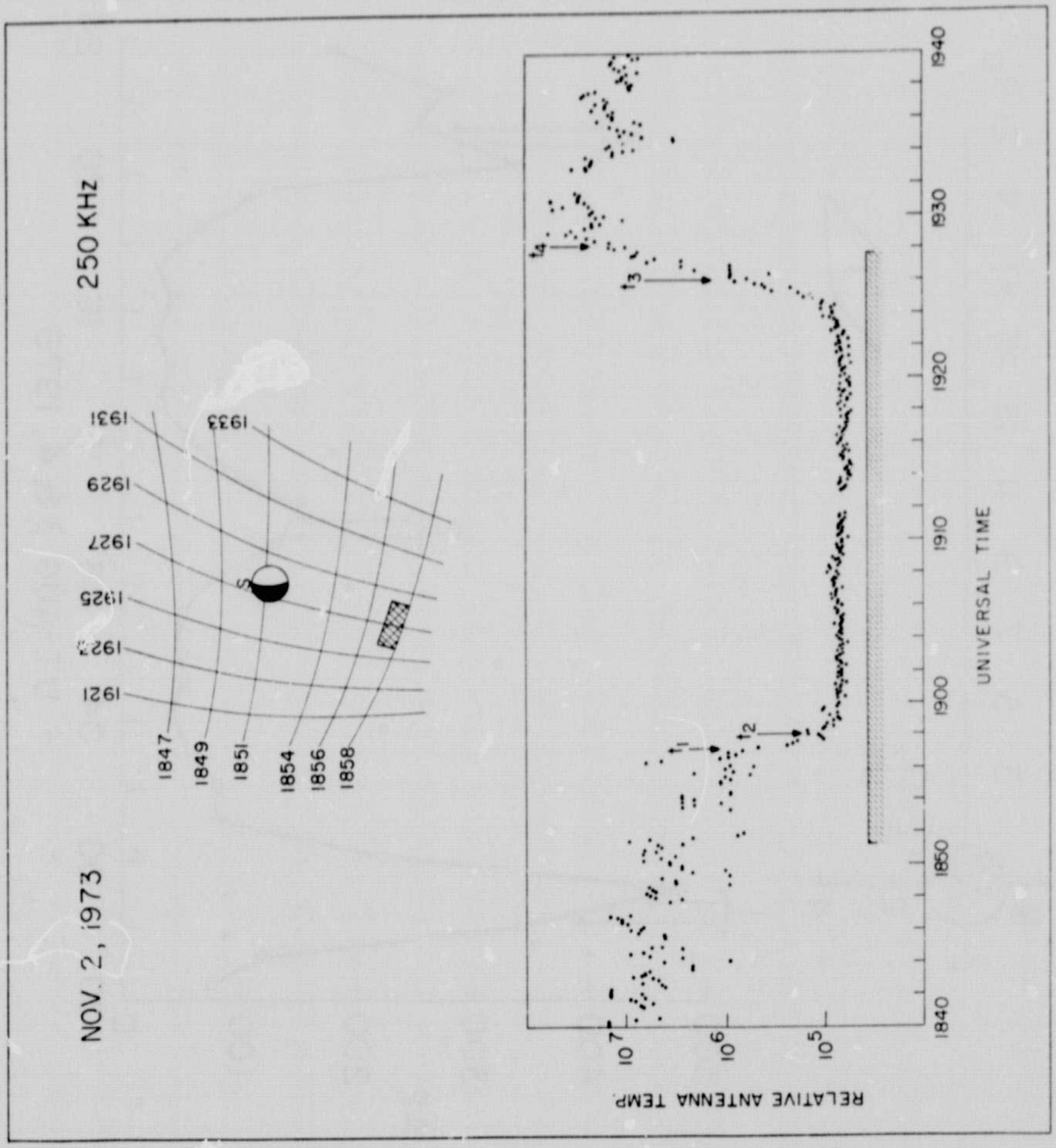

NOV. 2, 1973
250 KHz
1921
1923
1925
1927
1929
1931
1933
1847
1849
1851
1854
1856
1858
S
t_1
t_2
t_3
t_4
10^7
10^6
10^5
RELATIVE ANTENNA TEMP.
1840
1850
1900
1910
1920
1930
1940
UNIVERSAL TIME

Figure 1

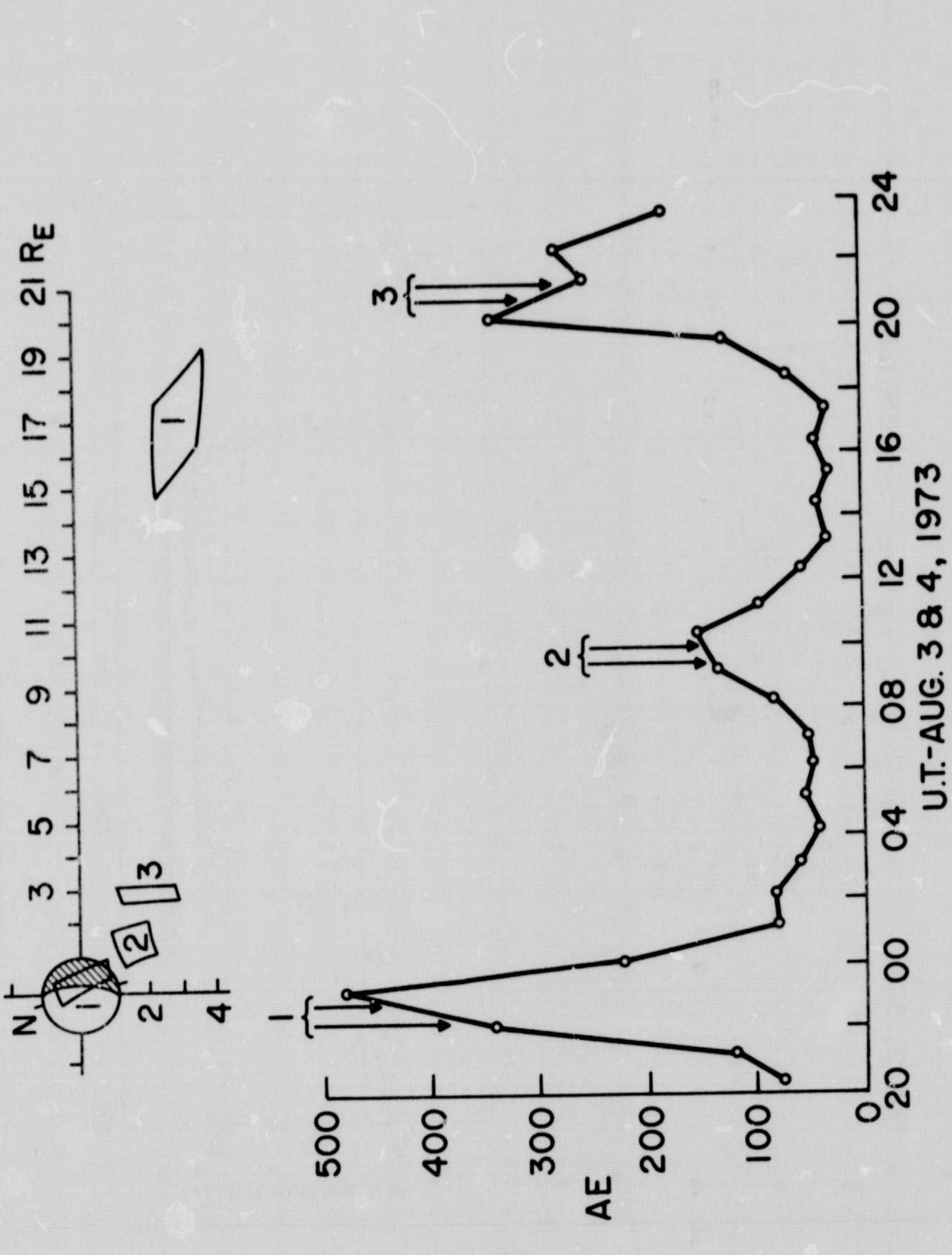

Figure 2a

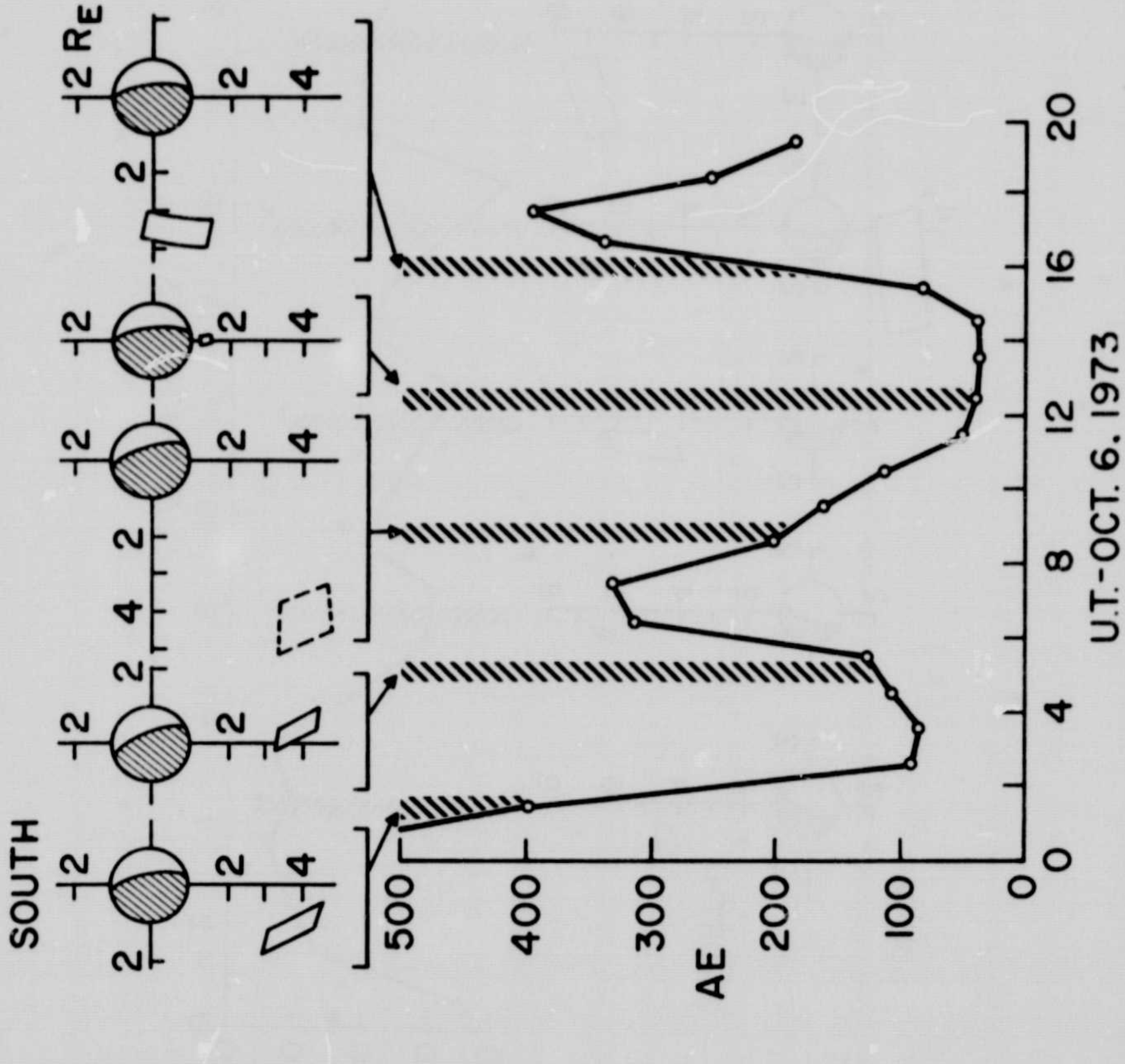

Figure 2b

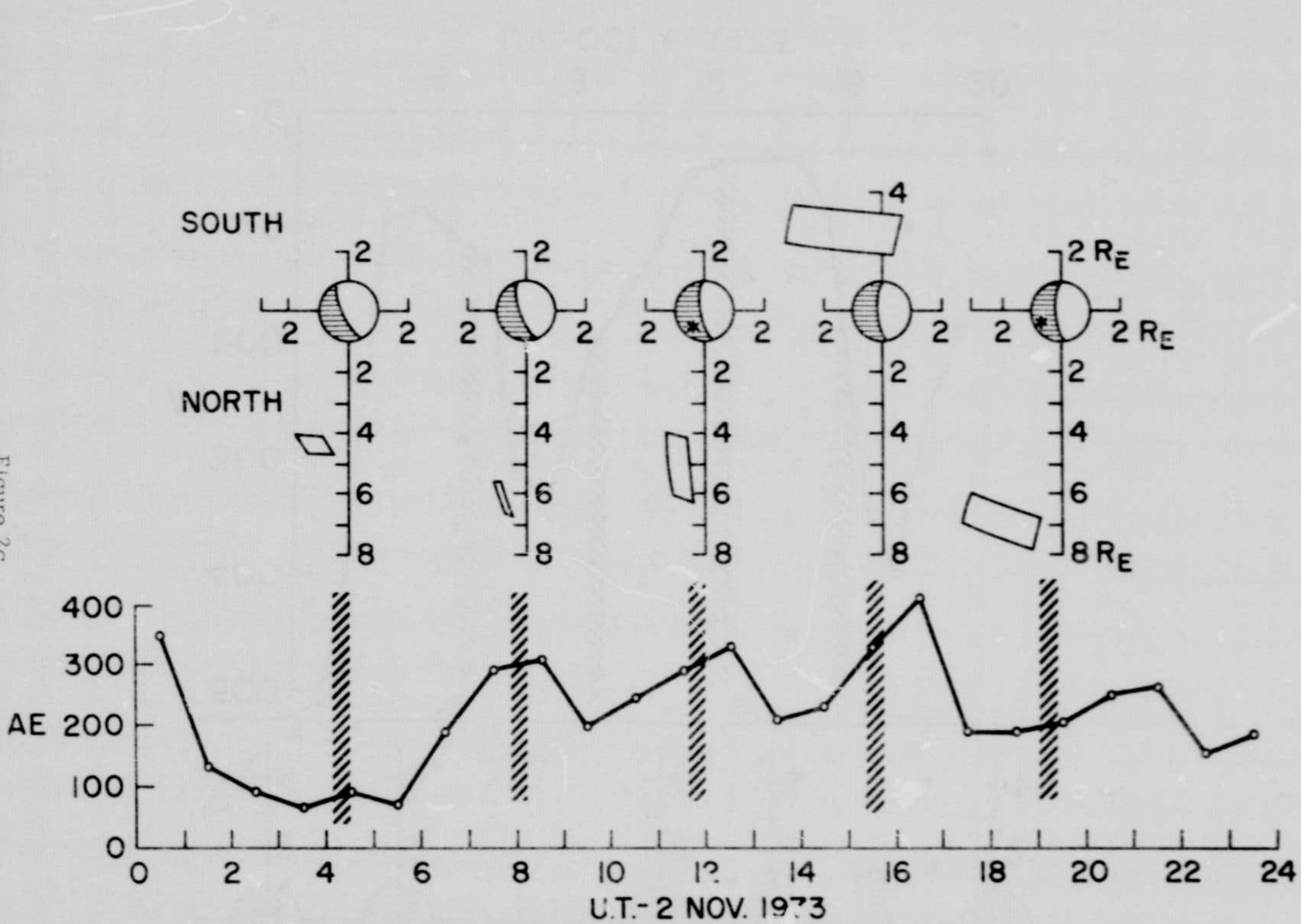

Figure 2c

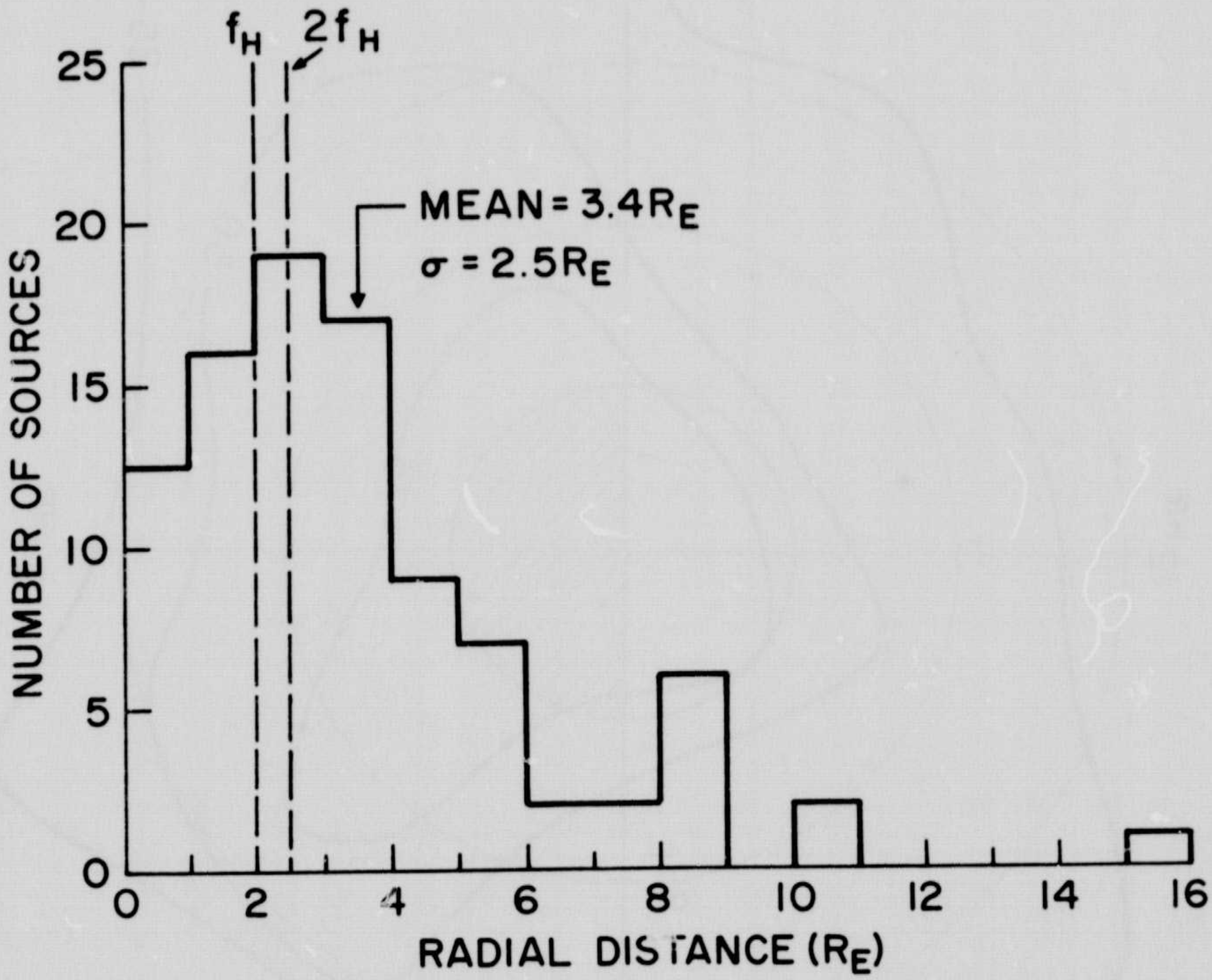

f_H
2f_H
MEAN = 3.4R_E
σ = 2.5R_E
NUMBER OF SOURCES
25
20
15
10
5
0
0
2
4
6
8
10
12
14
16
RADIAL DISTANCE (R_E)

Figure 3

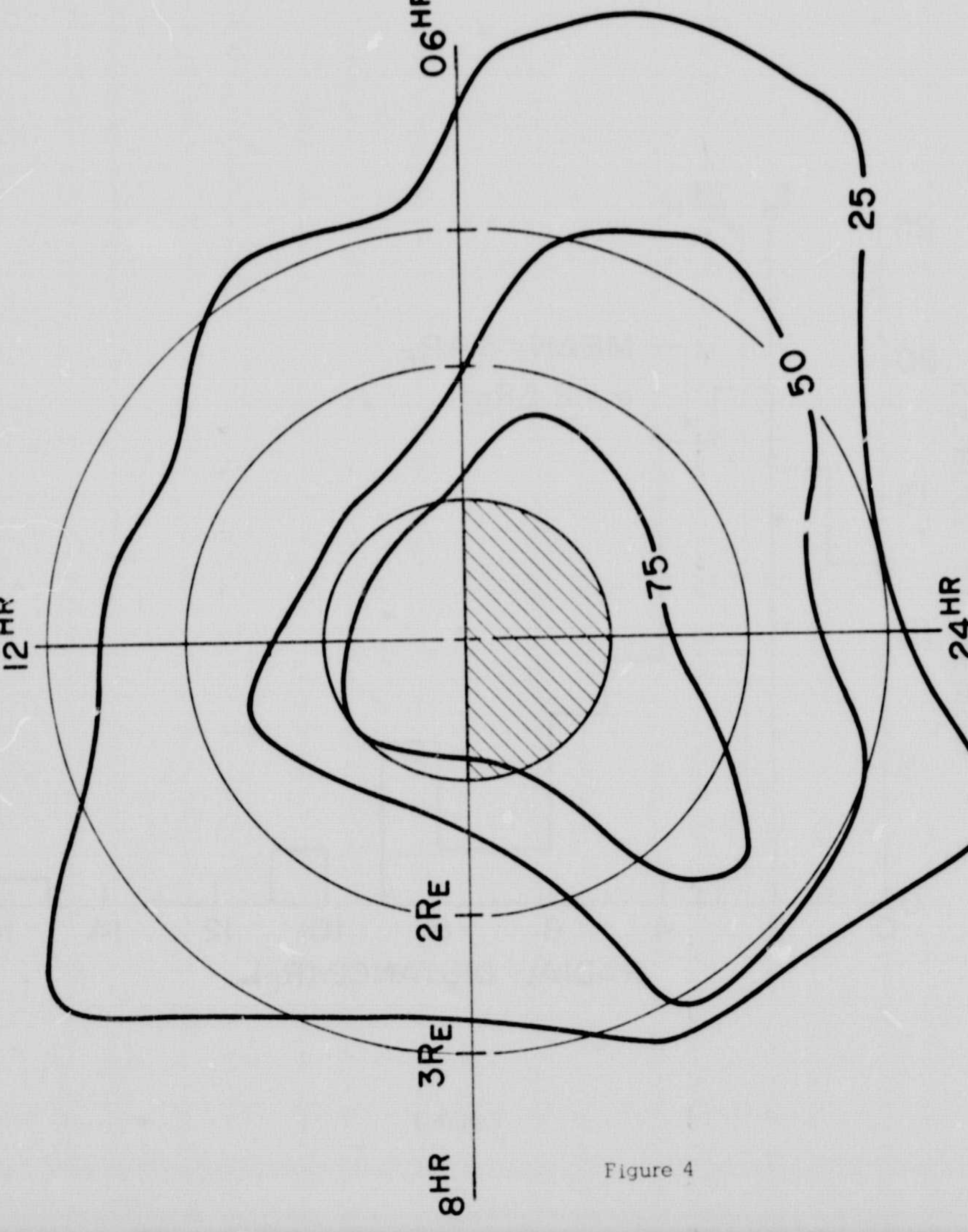

Figure 4